

Preparation and Catalytic Activity Comparison of Porous NiO, Co₃O₄ and NiCo₂O₄ Superstructures on the Thermal Decomposition of Ammonium Perchlorate

Jian-Guo Wang¹, Li-Na Jin^{1,*}, Xin-Ye Qian¹, and Ming-Dong Dong^{2,*}

¹*Institute for Advanced Materials, and School of Materials Science and Engineering,
Jiangsu University, Zhenjiang 212013, China*

²*Center for DNA Nanotechnology (CDNA), Interdisciplinary Nanoscience Center (iNANO),
Aarhus University, DK-8000 Aarhus, Denmark*

Porous NiO, Co₃O₄ and NiCo₂O₄ superstructures were successfully prepared via a facile hydrothermal-annealing method. The products were characterized by powder X-ray diffraction (XRD), field-emission scanning electron microscopy (FESEM) and energy dispersive spectrometry (EDS). The Brunauer-Emmett-Teller surface area and pore volume of the products were measured by N₂ adsorption isotherms. The catalytic performance of the as-prepared porous NiO, Co₃O₄ and NiCo₂O₄ superstructures on the thermal decomposition of ammonium perchlorate (AP) was investigated by thermal gravimetric analysis and differential scanning calorimeter. The results showed Co₃O₄ superstructures were more effective than others for the thermal decomposition of AP and the thermal decomposition temperature of AP shifted downward about 136.2 °C. Furthermore, the catalytic mechanism of porous NiO, Co₃O₄ and NiCo₂O₄ superstructures on the thermal decomposition of AP was discussed.

Keywords: Metal Oxide, Nanostructures, Thermal Decomposition, Ammonium Perchlorate.

1. INTRODUCTION

Solid fueled rockets are widely used in the fields of aerospace, universal exploration and satellite launching. Ammonium perchlorate (AP) is an important oxidizer in solid composite propellants for solid fueled rockets and its content is about 60% ± 90% by weight. The combustion behavior of propellants is highly relevant to the thermal decomposition of AP. The lower temperature at which AP begins to decompose, the higher the burning rate of propellants is.^{1–3} Therefore, catalyzed thermal decomposition of AP has attracted a great deal of attention in the past decades.^{4–7}

Recently, transition metal oxides and their compounds nanomaterials with various morphologies have been used as effective catalyst for thermal decomposition of AP, including CoO nanocrystals,⁸ CuO nanorods,⁹ α-Fe₂O₃ nanotubes,¹⁰ Fe₂O₃ nanorods and micro-octahedrons,¹¹ α-MnO₂ nanowires,¹² V₂O₅ nanowires,¹³ octahedral

Co₃O₄ nanoparticles,¹⁴ CuFe₂O₄ nanoparticles¹⁵ etc. It is well known that the catalytic activity of metal oxides and their compounds is closely related to their surface area and pore volume. Superstructures with higher BET and pore volume have been great interest in the past decade due to their potential applications in many fields.^{16–21} According to the past literature, porous transition metal oxide superstructures could have better catalyst effect for thermal decomposition of AP.^{22–25} For example, Jia et al. prepared porous ZnCo₂O₄ nanorods catalyst which decreased the decomposition temperature (*T_d*) of AP from approximately 315 °C and 450 °C to 274.5 °C and 290.9 °C.²² Moreover, they produced porous CoFe₂O₄ superstructures which decreased *T_d* of AP to 290.3 °C and 319.6 °C.²³ In addition, in our past works, we prepared porous Co₃O₄ and NiO superstructures using metal organic frameworks (MOFs) as precursors and found that they had good catalytic effect for the decomposition of AP.^{24, 25} However, to the best of our knowledge, there are still few reports on the comparative investigations of catalytic

*Authors to whom correspondence should be addressed.

behaviors of porous transition metal oxides and their compounds superstructures for thermal decomposition of AP.

In recent decades, the hydrothermal method has been widely used for the synthesis of a variety of functional nanomaterials with specific sizes and shapes and it possesses many advantages, such as fast reaction kinetics, short processing time, phase purity, and high crystallinity.^{26,27} In the present work, we successfully synthesized NiO, Co₃O₄ and NiCo₂O₄ superstructures via a facile and economical hydrothermal-annealing method without the assistance of template or surfactant. The catalytic effect of the prepared NiO, Co₃O₄ and NiCo₂O₄ superstructures on the thermal decomposition of AP was studied by thermal gravimetric analysis (TGA) and differential scanning calorimeter (DSC) in detail.

2. EXPERIMENTAL DETAILS

2.1. Synthesis of Porous NiO, Co₃O₄ and NiCo₂O₄ Superstructures

All chemicals and solvents are of analytical grade and were used as received without further purification. In a typical experiment, NiCl₂·6H₂O, CoCl₂·6H₂O and 3 mmol of urea was dissolved in 20 mL de-ionized water to form a solution, in which the total molar mass of NiCl₂·6H₂O and CoCl₂·6H₂O is 1 mmol. The Ni/Co molar ratio is 1:0, 0:1 and 1:2, respectively. Subsequently, the as-prepare solution was transferred into a 25 mL Teflon-lined stainless steel autoclave, and maintained at 120 °C for 5 h. After the autoclave was allowed to cool at room temperature, the product was collected by centrifugation, and washed with deionized water and alcohol for several times, and dried in oven at 60 °C for 5 h. In addition, a calcination process (350 °C for 2 h in air with a heating rate of 2 °C min⁻¹) was performed to transform precursor to NiO, Co₃O₄ and NiCo₂O₄ crystals.

2.2. Catalytic Activity Tests

The catalytic activities of porous NiO, Co₃O₄ and NiCo₂O₄ superstructures in the thermal decomposition of AP were studied by a differential scanning calorimeter (DSC) and thermogravimetric analysis (TGA) using STA 449C thermal analyzer with a heating rate of 10 °C min⁻¹ in N₂ atmosphere over the temperature range of 30–500 °C. Before the experiments, the as-prepared porous NiO, Co₃O₄ and NiCo₂O₄ products were mixed with AP and ground at a mass ratio of 98:2 to prepare the target samples for thermal decomposition analyses.

2.3. Characterization

The products were characterized by powder X-ray diffraction (XRD) on a Rigaku D/max 2500PC diffractometer with graphite monochromator and Cu K_α radiation

($\lambda = 0.15406$ nm) at a step width of 0.02°. SEM images and EDS of the products were obtained on a field emission scanning electron micro analyzers (JSM-7001F), employing an accelerating voltage of 5 kV or 20 kV. Nitrogen adsorption–desorption isotherms, pore size distributions and surface areas of the samples were measured by the instrument of NOVA 2000e using N₂ adsorption.

3. RESULTS AND DISCUSSION

3.1. Structure and Morphology of the As-Prepared Samples

Figure 1 shows the XRD patterns of the products after annealing treatment. All peaks in Figures 1(a)–(c) can be indexed as the cubic NiO, the cubic Co₃O₄ and the cubic NiCo₂O₄ phase by comparison with the JCPDS card files no. 78-0643, 78-1970 and 73-1702. No other impurity peaks are detected, indicating that NiO, Co₃O₄ and NiCo₂O₄ can be successfully obtained and all products are pure. Figure 2 depicts the EDS analyses of the as-prepared products. When the Ni/Co molar ratio in start materials is 1:1, the peaks of Ni, Co and O in the product can be easily found (Fig. 2(c)). The C, Si and Au peak can be attributed to CO₂ adsorbed by the sample, the substrate and the gold sputtering, respectively. Based on the calculation, the Co/Ni atomic ratio is 2.05, which is close to the stoichiometric ratio of NiCo₂O₄.

The morphologies of all the products are characterized by FESEM and the images of the samples are shown in Figure 3. When the Ni/Co molar ratio is 1:0, the results shown in Figure 3(a) reveal that NiO particles are composed of sphere-like architectures. Figure 3(c) shows the morphology of Co₃O₄ prepared in the presence of 1 mmol of CoCl₂·6H₂O. It was observed that Co₃O₄ consists of flower-like superstructures with abundant of nanorods. Figure 3(e) illustrates urchin-like superstructures for NiCo₂O₄ products. From the high-magnification SEM

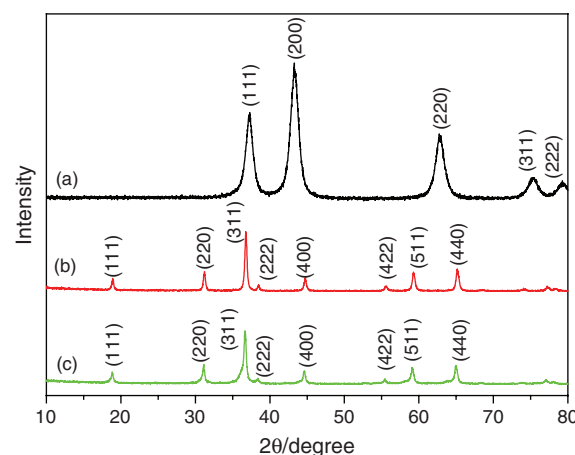


Figure 1. XRD patterns of the as-prepared (a) NiO, (b) Co₃O₄ and (c) NiCo₂O₄ superstructures.

images (Figs. 3(b), (d) and (f)), it can be clearly seen that a large number of cracks and pores exist on the surface of the products.

3.2. Catalytic Activity of Decomposing Ammonium Perchlorate

DSC curves for thermal decomposition of pure AP and its mixture with NiO, Co₃O₄ and NiCo₂O₄ superstructures are shown in Figure 4. Generally, the thermal decomposition of pure AP takes place in three steps: the

endothermic phase transition at 240–250 °C, the low-temperature decomposition (LTD) at 300–330 °C and the high-temperature decomposition (HTD) at 410–450 °C (Fig. 4(d)).¹⁰ When NiO, Co₃O₄ and NiCo₂O₄ superstructures as catalysts were added to AP, all samples have the similar endothermic peaks at about 250 °C, indicating that the catalysts have little effect on the crystallographic transition temperature of AP. However, in the relatively high temperature region, the samples containing catalysts have dramatic changes in the exothermic peaks of AP decomposition. When 2 wt% catalysts were added to AP, the original exothermic peak of pure AP at 445.0 °C disappeared and only one exothermic peak was observed. The exothermic peak temperature was 331.2, 308.8 and 335.1 °C for NiO, Co₃O₄ and NiCo₂O₄ superstructures, respectively (Figs. 4(a)–(c)).

The weight loss of AP is determined from the TG curves of different catalysts (Fig. 5). Figure 5(d) exhibits two weight loss steps while Figures 5(a)–(c) show only one weight loss step. Obviously, when catalysts were added to AP, the final decomposition temperature is decreased from 450.4 °C (pure AP) to 352.8 °C (NiO), 313.8 °C (Co₃O₄) and 338.6 °C (NiCo₂O₄), respectively. The results are in agreement with those of the DSC curves shown in Figure 4. From the above experimental results, it was found that NiO and Co₃O₄, and NiCo₂O₄ superstructures had good catalytic properties and Co₃O₄ superstructures had the most effective catalytic activity for the thermal decomposition of AP. The catalytic activity of Co₃O₄ superstructures was higher than that of Co₃O₄ nanoparticles, nanosheets and cubes.^{14, 24, 28}

3.3. Catalytic Mechanism of Decomposing Ammonium Perchlorate

Up to now, the mechanism of the thermal decomposition of AP is still unclear because the decomposition process is a complex hetero-phase process involving coupled reactions in the solid, absorbed and gaseous phases.²² According to the traditional electron-transfer theory, the presence of partially filled 3d orbit in Ni²⁺ or Co³⁺ provides help in an electro-transfer process. Positive hole in *p*-type semiconductor oxides like NiO, Co₃O₄ and NiCo₂O₄, which can accept electrons from AP ion and its intermediate products, enhance the thermal decomposition of AP.^{29, 30} Generally, there are many factors influencing the catalytic effect of the *p*-type semiconductor oxides on the thermal decomposition of AP, such as chemical nature, particle size, morphology and surface area.^{24, 31–33} In our present work, the BET surface areas and pore volumes of NiO, Co₃O₄ and NiCo₂O₄ superstructures are 54 m² g⁻¹ and 121.6 mm³ g⁻¹, 26 m² g⁻¹ and 106.2 mm³ g⁻¹, 69 m² g⁻¹ and 157.2 mm³ g⁻¹, respectively. The average particle sizes of NiO, Co₃O₄ and NiCo₂O₄ superstructures are calculated by the Debye-Scherrer formula to be about 6.9 nm, 24.4 nm and 22.3 nm, respectively. However, Co₃O₄ superstructures with smaller surface area and larger particle size

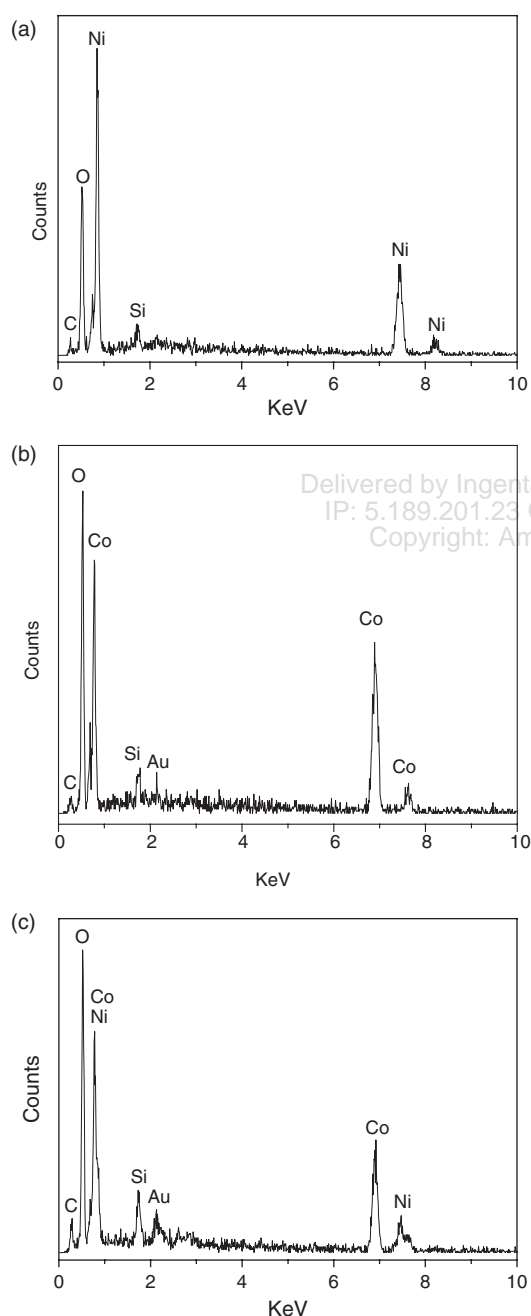


Figure 2. EDS spectra of the as-prepared (a) NiO, (b) Co₃O₄ and (c) NiCo₂O₄ superstructures.

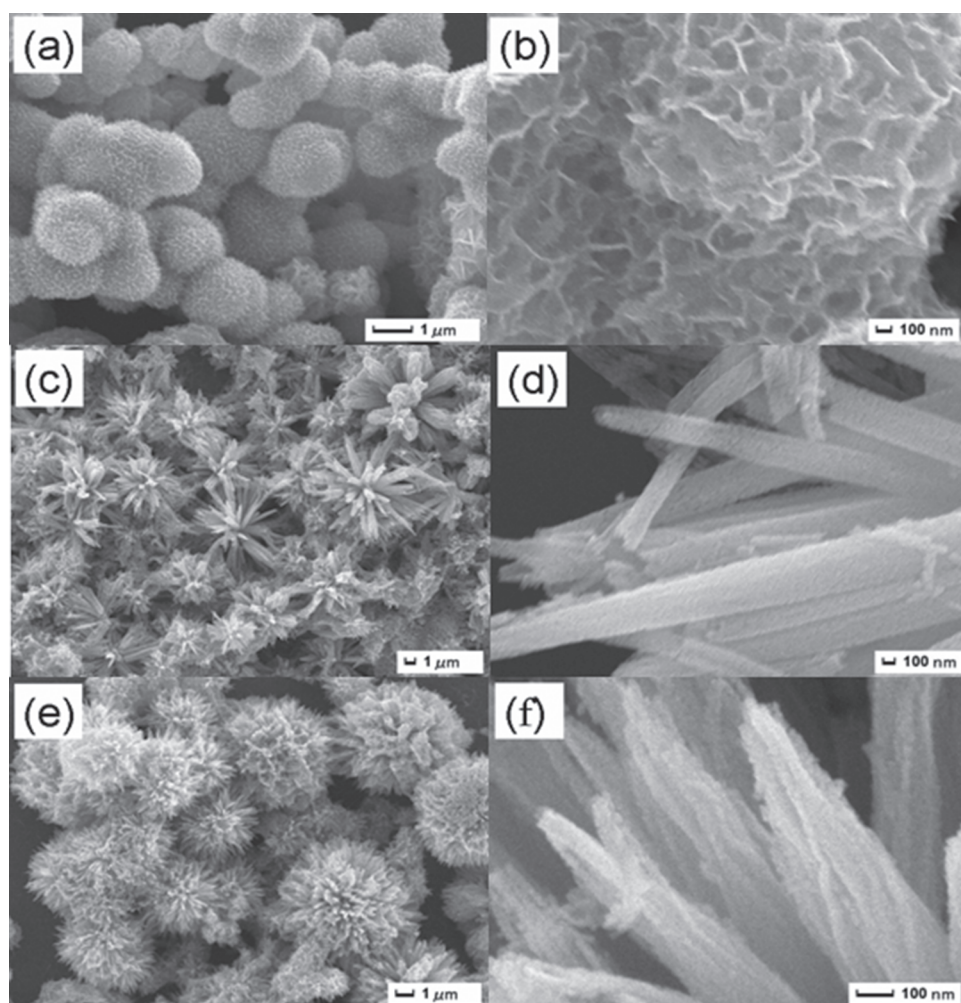


Figure 3. SEM images of (a), (b) NiO, (c), (d) Co₃O₄ and (e), (f) NiCo₂O₄ superstructures.

were more effective than others for the thermal decomposition of AP. In addition, Co₃O₄ superstructures had a higher catalytic activity than NiCo₂O₄ superstructures which had the similar morphology with Co₃O₄ superstructures.

This indicates that the catalytic ability of the as-prepared products for decreasing the decomposition of AP depend on not only their surface area, particle size and morphology but also their chemical nature. Thus, the high

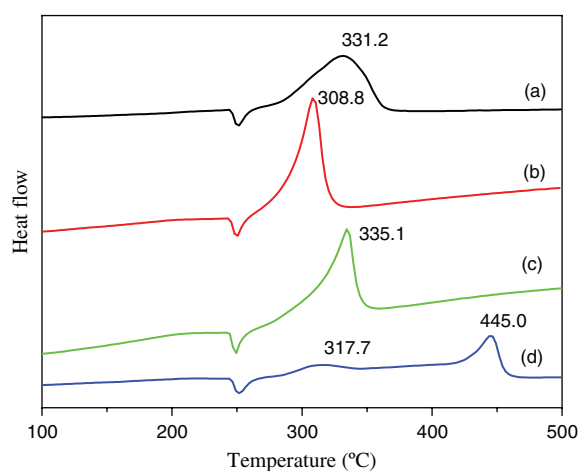


Figure 4. DSC curves of the AP samples after addition of (a) 2 wt% NiO, (b) 2 wt% Co₃O₄, (c) 2 wt% NiCo₂O₄ superstructures and (d) pure AP.

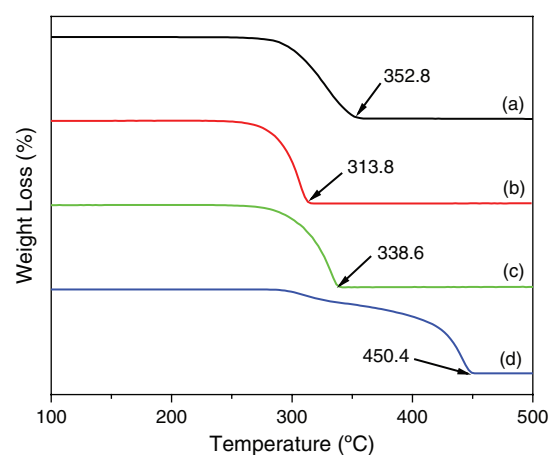


Figure 5. TG curves of the AP samples after addition of (a) 2 wt% NiO, (b) 2 wt% Co₃O₄, (c) 2 wt% NiCo₂O₄ superstructures and (d) pure AP.

catalytic performance of porous Co₃O₄ superstructures may be explained as that in the decomposition process of AP, Co₃O₄ provides a bridge for transferred electrons from perchlorate ions to ammonium ions better than other two metal oxides.²⁸

4. CONCLUSION

In summary, we synthesized porous NiO, Co₃O₄ and NiCo₂O₄ superstructures via a facile and economical hydrothermal-annealing method without the assistance of template or surfactant. The as-prepared porous NiO, Co₃O₄ and NiCo₂O₄ superstructures have good catalytic properties for the thermal decomposition of AP due to their large BET surface area and pore volume. Co₃O₄ superstructures show better catalytic activity than others and shifted the AP thermal decomposition temperature downwardly to about 136.2 °C. The mechanism based on traditional electron-transfer theory was proposed for the thermal decomposition of AP in the presence of porous transition metal oxides and their compounds superstructures.

Acknowledgments: We acknowledge the financially supported by National Natural Science Foundation of China (No. 21401081), China Postdoctoral Science Foundation (No. 2014M560397), Jiangsu Natural Science Funds for Distinguished Young Scholars (No. BK20140013), Jiangsu Postdoctoral Science Foundation (No. 1401051C) and the Senior Intellectuals Fund of Jiangsu University (No. 14JDG058 and 11JDG098).

References and Notes

1. M. Zou, X. Jiang, L. Lu, and X. Wang, *J. Hazard. Mater.* 225, 124 (2012).
2. G. Tang, S. Tian, Z. Zhou, Y. Wen, A. Pang, Y. Zhang, D. Zeng, H. Li, B. Shan, and C. Xie, *J. Phys. Chem. C* 118, 11833 (2014).
3. X. Guan, L. Li, J. Zheng, and G. Li, *RSC Adv.* 1, 1808 (2011).
4. M. Zou, X. Wang, X. Jiang, and L. Lu, *J. Solid State Chem.* 213, 235 (2014).
5. C. Xu, X. Wang, J. Zhu, X. Yang, and L. Lu, *J. Mater. Chem.* 18, 5625 (2008).
6. N. Li, M. Cao, Q. Wu, and C. Hu, *Cryst. Eng. Comm.* 14, 428 (2012).
7. W. Zhang, P. Li, H. Xu, R. Sun, P. Qing, and Y. Zhang, *J. Hazard. Mater.* 268, 273 (2014).
8. L. Li, X. Sun, X. Qiu, J. Xu, and G. Li, *Inorg. Chem.* 47, 8839 (2008).
9. L. Chen, L. Li, and G. Li, *J. Alloys Comp.* 464, 532 (2008).
10. L. Song, S. Zhang, B. Chen, J. Ge, and X. Jia, *Colloid Surf. A-Physicochem. Eng. Asp.* 360, 1 (2010).
11. H. Xu, X. Wang, and L. Zhang, *Powder Technol.* 185, 176 (2008).
12. L. Chen and D. Zhu, *Solid State Sci.* 27, 69 (2014).
13. Y. Zhang, N. Wang, Y. Huang, W. Wu, C. Huang, and C. Meng, *Ceram. Int.* 40, 11393 (2014).
14. H. Zhou, B. Lv, D. Wu, and Y. Xu, *Cryst. Eng. Comm.* 15, 8337 (2013).
15. T. Liu, L. Wang, P. Yang, and B. Hu, *Mater. Lett.* 62, 4056 (2008).
16. B. Gao, H. Fu, Y. Chen, and Z. Gu, *J. Nanosci. Nanotechnol.* 12, 8067 (2012).
17. R. Mallampati and S. Valiyaveetil, *J. Nanosci. Nanotechnol.* 12, 618 (2012).
18. J. Wu and D. Xue, *Nanosci. Nanotechnol. Lett.* 3, 317 (2011).
19. B. Jia, W. Jia, X. Wu, and F. Qu, *Sci. Adv. Mater.* 4, 1127 (2012).
20. Y. Z. Zhang, Y. Wang, Y. L. Xie, T. Cheng, W. Y. Lai, H. Pang, and W. Huang, *Nanoscale* 6, 14354 (2014).
21. H. B. Wu, H. Pang, and X. W. Lou, *Energy Environ. Sci.* 6, 3619 (2013).
22. Z. Jia, D. Ren, Q. Wang, and R. Zhu, *Appl. Surf. Sci.* 270, 312 (2013).
23. Z. Jia, L. Yang, Q. Wang, J. Liu, M. Ye, and R. Zhu, *Mater. Chem. Phys.* 145, 116 (2014).
24. L. N. Jin, Q. Liu, and W. Y. Sun, *Cryst. Eng. Comm.* 14, 7721 (2012).
25. L. N. Jin, Q. Liu, and W. Y. Sun, *Chin. Chem. Lett.* 24, 663 (2013).
26. M. R. Gao, Y. F. Xu, J. Jiang, and S. H. Yu, *Chem. Soc. Rev.* 42, 29 (2012).
27. M. K. Devaraju and I. Honma, *Adv. Energy Mater.* 2, 284 (2012).
28. E. A. Gheshlaghi, B. Shaabani, A. Khodayari, Y. A. Kalandaragh, and R. Rahimi, *Powder Technol.* 217, 330 (2012).
29. S. Chaturvedi and P. N. Dave, *J. Sa. Chem. Soc.* 17, 135 (2013).
30. D. Zhang, Q. Xie, A. Chen, M. Wang, S. Li, X. Zhang, G. Han, A. Ying, J. Gong, and Z. Tong, *Solid State Ionics* 181, 1462 (2010).
31. Y. Zhang, X. Liu, J. Nie, L. Yu, Y. Zhong, and C. Huang, *J. Solid State Chem.* 184, 387 (2011).
32. Z. T. Liu, X. Li, Z. W. Liu, and J. Lu, *Powder Technol.* 189, 514 (2009).
33. I. P. S. Kapoor, P. Srivastava, and G. Singh, *Propellants Explos. Pyrotech.* 34, 351 (2009).

Received: 1 March 2015. Accepted: 23 April 2015.